

Article

Multiple Effects of Topographic Factors on Spatio-temporal Variations of Vegetation Patterns in the Three Parallel Rivers Region, Southeast Tibet

Chunya Wang^{1,2,3}, Jinniu Wang^{1,2 *}, Niyati Naudiyal¹, Ning Wu¹, Xia Cui⁴, Yanqiang Wei⁵, Qingtao Chen³

¹ Chengdu Institute of Biology, Chinese Academy of Sciences, Chengdu 610041; wangcy9610@gmail.com (C.W.); naudiyal.niyati@gmail.com(N.N.); wuning@cib.ac.cn(N.W.)

² Mangkang ecological monitoring station, Tibet ecological security barrier ecological monitoring network, Changdu 854000;

³ Earth Sciences College, Chengdu University of Technology, Chengdu 610059; cqt@cdut.edu.cn(Q.C.)

⁴ School of Resources and Environmental Sciences, Lanzhou University, Lanzhou 730000; xiacui@lzu.edu.cn(X.C.)

⁵ Northwest Institute of Eco-Environment and Resources, Chinese Academy Sciences, Lanzhou 730000; weiyq@lzb.ac.cn(Y.W.)

* Correspondence: wangjn@cib.ac.cn

Abstract: Topographic factors are recognized as one of the key factors influencing vegetation distribution patterns, and studying the interactions between them can contribute to enhancing our understanding of future vegetation dynamics. We used the Moderate-resolution Imaging Spectroradiometer Normalized Differential Vegetation Index (MODIS NDVI) image dataset (2000-2019), combined with Digital Elevation Model (DEM), and vegetation type data for trend analysis, and explored NDVI variation and its relationship with topographic factors through an integrated geographically-weighted model in the Three Parallel Rivers Region (TPRR) of southeastern Tibetan plateau in the past 20 years. Our results indicated that there was no significant increase of NDVI in the entire basin between 2000-2019, except for the Lancang River basin. In the year 2004, abrupt changes in NDVI were observed across the whole basin and each sub-basin. During 2000-2019, the mean NDVI value of the whole basin increased initially and then decreased with the increasing elevation. However, it changed marginally with changes in slope and aspect. We observed a distinct spatial heterogeneity in vegetation patterns with elevation, with vegetation in the southern regions showing higher NDVI than the north as a whole. Most of the vegetation cover was concentrated in the slope range of 8~35°, with no significant difference in distribution except flat-land. Furthermore, from 2000 to 2019, the vegetation cover in the TPRR showed an improving trend with the changes of various topographic factors, with the largest improvement area (36.10%) in the slightly improved category. The improved region was mainly distributed in the source area of the Jinsha River basin and the southern part of the whole basin. Geographically weighted regression (GWR) analysis showed that elevation was negatively correlated with NDVI trends in most areas, especially in the middle reaches of Nujiang River basin and Jinsha River basin, where the influence of slope and aspect on NDVI change was considerably much smaller than elevation.

Keywords: MODIS NDVI; Vegetation cover; Trend analysis; Sen+Mann-Kendall; Topography; GWR; Qinghai-Tibetan Plateau

1. Introduction

Being an important component of terrestrial ecosystems, vegetation plays a crucial role in maintaining ecosystem stability [1, 2]. The dynamics of vegetation patterns is a complex and prolonged process, driven by multiple biotic and anthropogenic factors such as climate change, land use change, and ecological engineering measures amongst others

[3]. Being one of the most fragile terrestrial ecosystems, mountainous ecosystem are rather sensitive to global climatic change and human activities. Large vertical gradient and unique topographical conditions make mountainous regions the most abundant land unit on the earth and a key area for global biodiversity conservation [4, 5]. As an important component of mountain ecosystem, vegetation cover change has a more significant feedback on climate and other factors than plain area. Therefore, the analysis of the process and driving factors of mountain vegetation dynamics has always been a key concern amongst global climatic change and mountain research community [6, 7].

The topographic variability in mountain ecosystems and resulting microclimates influence the variations in regional vegetation patterns thereby supporting high levels of biodiversity [5]. In recent years, international research on mountain vegetation has broadened from earlier studies that focused mostly on temperate zones of Europe (e.g., the Alps and the Scandes) [8] to other mountainous regions in the world including Alaska and the State of California, and the Rocky Mountains in North America [9, 10], tropical mountainous regions of Africa (Kenya, Mount Kilimanjaro, Mount Wilhelm in New Guinea, etc.) [11, 12], the subtropical Andean regions [13, 14], and the southern and eastern Himalayas [15]. Meanwhile, research field has also expanded from the physiological ecology of alpine plants to issues of elevational zonality and impact of global climate change of alpine vegetation patterns [16, 17]. In particular, studies of alpine vegetation in the eastern Himalayas and the Tibetan Plateau has made great progress in recent years through the efforts of scholars in China, who studied the vegetation pattern in the Three River Headwater Region, Hengduan Mountains, Tianshan Mountains, Changbai Mountains and Qinling Mountains, and deliberated the response mechanisms for conservation of mountain vegetation in the face of global climate change [18-21].

Several environmental factors have been widely identified as drivers for vegetation cover changes. Natural (e.g., climatic factors, topography and etc.) and social factors (e.g., socio-economics, ecological engineering policies and settlements) can have a strong influence on vegetation growth processes, the extent of which varies from one places to another [5, 22]. Most studies believe that precipitation and temperature are the main climatic factors affecting regional vegetation change [23], in addition to topography [24]. In mountainous areas with complex topography, topographic features (elevation, slope, aspect, etc.) have noticeable effects on vegetation patterns by themselves but also by controlling other environmental factors, such as solar radiation, wind, precipitation, snow cover, and edaphology distribution, a combination of these environmental factors jointly determines the spatial heterogeneity of vegetation pattern [17, 19]. Besides, human activities (such as roads, settlements and hydraulic engineering) also have an impact on mountain vegetation cover [22], which may have a negative impact on vegetation in low elevation regions, while less interference on the vegetation in the middle elevation [7, 25]. In the context of global climate change, topography is the only relatively constant environmental factor, and deeper insights on how topography controls the vegetation change pattern is particularly necessary to understand the vegetation dynamics and strengthen the response analysis of vegetation growth and distribution to topographic factors.

At present, the analysis of drivers affecting vegetation patterns in the Tibetan Plateau region is mostly concentrated in the analysis of climatic factors, and relatively little research has been conducted on topographic control mechanisms [24, 26, 27]. Given the inaccessibility of most mountainous regions, remote sensing (RS) and geographic information system (GIS) technology stand out as powerful tools for monitoring vegetation cover changes in mountainous areas by providing continuous, spatially detailed satellite data on mountainous vegetation cover [28]. With the development of RS technology, the types of remote sensing sensors have become more and more diversified, and the large-scale long time series vegetation dynamics has gradually developed into a hot spot for global change research, among which MODIS vegetation cover product data is regarded as one of the most effective data products for vegetation productivity analysis [29]. NDVI

has been proved to be a comprehensive index to describe the ecological functional characteristics of vegetation growth, net primary productivity and phenology at regional, continental and global scales [22, 30]. So far, it has been widely used to detect the response of vegetation dynamics to climate change, human activities and other driving factors at multiple spatio-temporal scales [31, 32]. Furthermore, the ordinary least square regression (OLS) analysis in the traditional model is a classic statistical method to estimate the relationship between independent variables and dependent variables, with an assumption of a spatially stationary relationship between dependent variables and independent variables, i.e., without spatial heterogeneity. However, a large number of studies have shown a significant spatial difference in model parameters [33], while geographical weighted regression (GWR) model has improved the traditional model by combining spatial correlation with linear regression, which can solve the problem of spatial heterogeneity effectively. By calculating the local parameters of the regression model, it can optimize the fitting effect of the model, so that the relationship between variables can vary depending on the change of geographical location, and better reflect the spatial non-stationarity of the relationship between NDVI and driving factors [34]. Such an approach is suitable for analyzing the dynamics of vegetation from inaccessible mountainous regions with remarkable accuracy. An example of such a terrain is the Qinghai-Tibet Plateau.

Hengduan Mountains, located in the southeastern margin of the Qinghai-Tibet Plateau, is an important ecological barrier area in the upper reaches of the Yangtze River between the transition zone of the first and second step of China's topography. The high elevation difference between mountains and valley floors including the complex and diverse geomorphological types in this region make it one an ideal natural laboratory with complex natural environment, fragile ecology and frequent natural disasters. Due to the influence of the Indian Ocean and Pacific monsoon circulation, the dry and wet seasons are obvious in the regional valleys.

The TPRR, located in the heart of the Hengduan Mountains in the southeastern Tibetan Plateau, has paid widespread attention for being a world-renowned scenic spot and World Natural Heritage Site. The region is characterized by paralleling alternately high mountains and canyons, and the effect of topographic elevation differences makes the vertical temperature changing significantly. The biodiversity in this area is incredibly rich due to the interaction of topographical and climate factors. Exploring unique geographical environment and vertical zone spectrum of multi-bioclimatic in the mountainous area favors our understanding of regional biodiversity, ecosystem functions and services, vegetation restoration and reconstruction as well as other issues. In the context of global change, mountain ecosystem is the signal "amplifier" of biological response to global change [4, 35]. Vegetation change in the region is a result of the interaction between natural conditions and human society. Therefore, it is particularly important to explore these variations and patterns to address driving factors of the mountainous vegetation under global climate change in the future.

Existing studies from the TPRR mainly focus on geology, dynamic changes of alpine vegetation, land use/cover changes, and biodiversity conservation [36-39], and tourism resources [40-42]. Although few scholars have studied vegetation changes and its driving factors analysis in the whole basin of the TPRR [43], studies in various sub-basins (e.g., Lancang river and Jinsha river basins and etc.) have found that both of the vegetation dynamics in the Jinsha River Basin and the Lancang River Basin are jointly affected by temperature and precipitation, the influence of precipitation is more significant in the Jinsha River Basin, while in the Lancang River Basin is more sensitive to temperature [44-46]. Furthermore, anthropological factors such as the establishment of large dams and reservoirs, hydropower stations, and the implementation of ecological projects have great and obvious specific effects on the vegetation pattern of basin [2]. Only a few scholars highlight the relationship between vegetation change and meteorological factors in the source areas of the Three Parallel Rivers, which confirmed increasing vegetation cover with significant correlation with air temperature in this area [43]. The TPRR is one of the

important ecological barriers and water resources conservation areas in China. In addition, there are unique arid valleys with distinct topography difference. Therefore, it is of vital importance to understand the influence of topographic factors on vegetation cover in this unique geographical unit. Therefore, based on the MODIS NDVI image data from 2000 to 2019, and combined with DEM as well as vegetation type data for trend method and geographically weighted model, this paper discusses the spatiotemporal dynamic changes of vegetation and its response to topographic factors (i.e. elevation, slope, aspect and other factors) in the TPRR. Based on the spatial heterogeneity, the difference of vegetation restoration effect and its causes, and multiple drivers were analyzed by using the geographically weighted model. The specific research question addressed in this study include: 1) What are the dynamic characteristics of NDVI at spatial and temporal scale? 2)How do different topographic factors effect on vegetation pattern? 3)What is the overall performance of all topographic factors by generalized analysis in terms of Geographically Weighted Regression modelling?

2. Materials and Methods

2.1. Study Area

The TPRR (24°00' ~36°00' N, 90°20' ~102°20' E) is located in the Hengduan Mountains in southwest China, spanning four provinces, Qinghai, Sichuan, Yunnan, and Tibet, bordering Qinghai-Tibet border in the north, Sichuan-Yunnan border in the East, and China-Myanmar border in the west, with a total basin area is about 50.07 million km² (Figure 1). In this paper, the division of the study area is based on the watershed data provided by the Resource and Environment Science and Data Center of the Chinese Academy of Sciences(<https://www.resdc.cn>), coupled with the reference to the existing literature, using the 90m resolution DEM in the Geospatial Data Cloud (<http://www.gscloud.cn>) as the data source. A series of spatial data analysis using DEM dataset was performed to identify the fill, flow direction, and flow accumulation in the region which enabled us to finally determine the watershed scope of the TPRR [47-49]. Three major Asian rivers, the Yangtze (Jinsha River), the Mekong River (Lancang River) and the Salween River (Nujiang River), which run parallel through the longitudinal valleys from north to south, and the vertical elevation difference of the region is nearly 6000m [47]. The unique environmental gradients make this region rich in biodiversity, and it is one of the regions with most unique species diversity in China [50]. The vegetation types of the region comprise of temperate alpine meadow, temperate coniferous forest, and deciduous broad-leaved forest in the upper reaches to temperate and subtropical alpine deciduous shrubs and tropical and subtropical evergreen broad-leaved forest at lower altitudes. The southwest monsoon from the Indian Ocean dominates the regional climate bringing about moisture and heat along the valleys. Contrasting seasons of rain and drought characterize the typical climate in the valley region, rainy in summer and dry in winter, whose precipitation concentrates from June to September. The temperature ranges from warm subtropical in the valley to snow-covered mountain tops, with the intense foehn effects leading to hot and dry weather in the inland valley. The complex and diverse climatic conditions and geo-

morphic characteristics make the basin a typical area for global environmental change research.

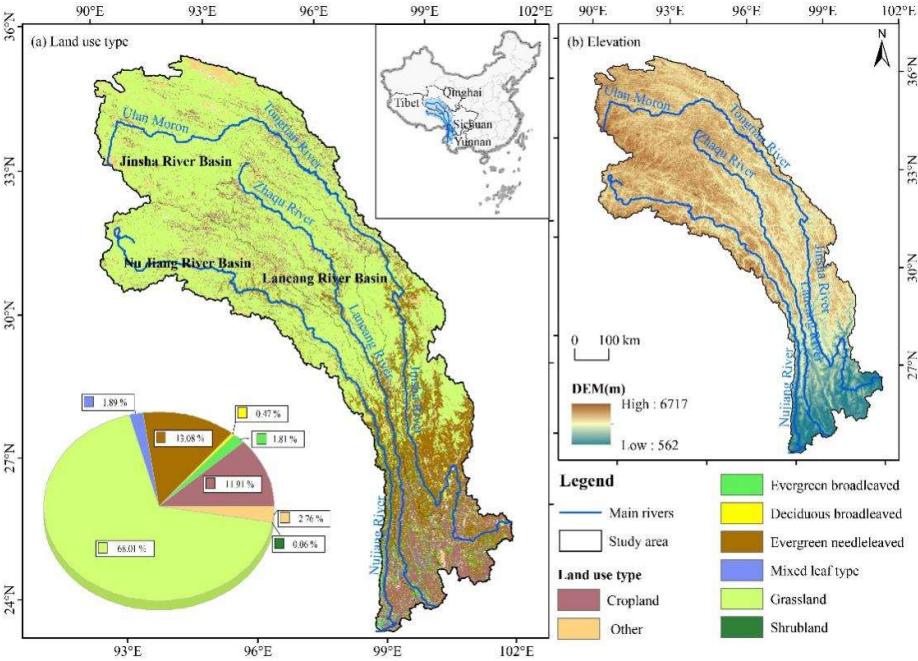


Figure1. The location and vegetation type map of the study area.

2.2. Data Sources and Preprocessing

2.2.1. Remote Sensing Data

NDVI data were provided by MODIS Terra (MOD13Q1) 16-day vegetation index product (2000-2019) from National Aeronautics and Space Administration (NASA), with a spatial resolution of 250m (available at <https://ladsweb.modaps.eosdis.nasa.gov/search/order/>). MODIS Reprojection Tool (MRT) was used to pre-process the original data (e.g. format and projection conversion, clipping, etc.). The maximum NDVI value was calculated using the maximum value composition method (MVC). Moreover, we obtained the best vegetation cover in this study area and further reduced the influence of clouds and atmospheric scattering. Finally, regions with NDVI value greater than 0.05 were identified as vegetated areas to avoid the interference of underlying surface information on NDVI of low vegetation cover area.

2.2.2. DEM Data

DEM data were collected from the Geospatial Data Cloud (<http://www.gscloud.cn>), with a resolution of 90m. According to the Chinese soil erosion classification standard and other references [51-53], we determined the characteristics of various terrain factors and then extracted the elevation, slope and aspect respectively from the DEM data for further analysis in ArcGIS10.2 (Figure 2, Table S1). In addition, spatial analysis tool was used to superimpose the terrain factors with the spatial distribution layers of NDVI to obtain the

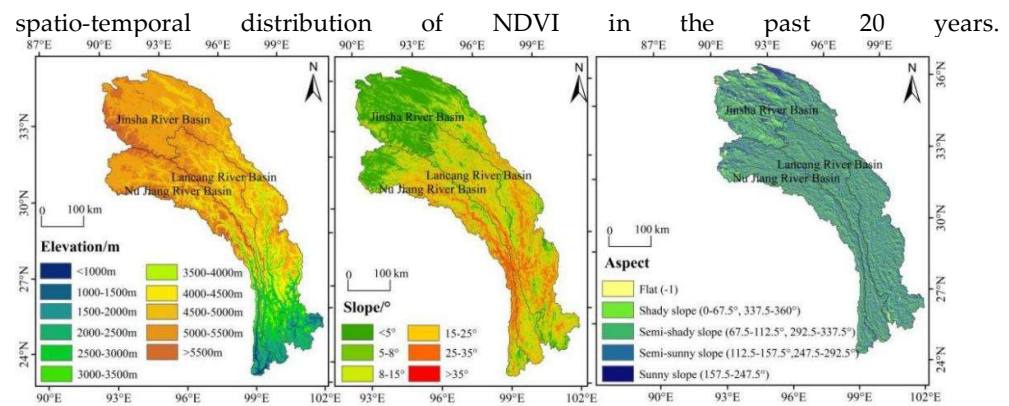


Figure 2. The hierarchical spatial distribution of topographic factors in the study area.

2.2.3. Vegetation Type Data

ESA CCI-LC land cover types were provided by the European space agency (<http://maps.elie.ucl.ac.be/CCI/viewer/>) with a 300 m spatial resolution. With more than 70% overall accuracy, the global ESA CCI-LC data has been widely used in land use/land cover dynamic studies, around the world monitoring [54-56]. In this region, the vegetation cover types mainly comprised of cropland, grassland, shrub grass, evergreen broad-leaved forest, deciduous broad-leaved forest, evergreen coniferous forest, and others (mainly water, bare land, snow and ice, etc.), a total of 7 categories [57, 58]. In order to minimize the impact of land use change on the distribution of vegetation types, the research methods of [59] were referred to extract the areas with unchanged vegetation types from 2000 to 2015 to represent the vegetation cover status in the study area in recent years.

2.3. Methods

2.3.1. Trend Analysis and Test

Firstly, monthly NDVI data were processed by maximum value composite (MVC) method to obtain maximum annual NDVI value, and the mean value method was applied to get the spatial distribution of mean NDVI in the study area. We divided NDVI datasets into 6 grades integrating the vegetation cover classification standard in the National Soil Erosion Classification Standard and the actual vegetation cover conditions in the TPRR [51], i.e., non-vegetation cover ($\text{NDVI} < 0.05$), low vegetation cover (NDVI between 0.05 and 0.30), medium and low vegetation cover (0.30 to 0.45), medium and high vegetation cover (0.45 to 0.60), medium and high vegetation cover (0.60 to 0.75), and high vegetation cover ($\text{NDVI} > 0.75$).

In order to study the variation characteristics of NDVI in the basin over time, the annual maximum NDVI values from 2000 to 2019 were selected to represent the vegetation cover in each year for inter-annual variation analysis in the basin.

Theil Sen and Mann-Kendall method have been widely used in meteorology and hydrology to the variation characteristics of NDVI analysis [30, 60]. Theil-Sen trend analysis method has a good ability to avoid outlier data disturbance or measurement error. The calculation method is as follows:

$$S_{\text{NDVI}} = \text{median} \frac{x_j - x_i}{j - i} (j > i > 1) \quad (1)$$

Where, x_i and x_j denote the i -th and j -th year time series data. $S_{\text{NDVI}} > 0$ indicates that the vegetation shows an upward trend, whereas the other indicates a downward trend. According to the results of Theil-Sen trend analysis, the change trend is divided into 5 levels. Meanwhile, Mann-Kendall method can test whether the trend is significant, and its calculation formula is as follows:

$$Z = \begin{cases} \frac{S-1}{\sqrt{\text{Var}(S)}} & (S > 0) \\ 0 & (S = 0) \\ \frac{S+1}{\sqrt{\text{Var}(S)}} & (S < 0) \end{cases} \quad (2)$$

$$\text{Among them, } S = \sum_{i=1}^{n-1} \sum_{j=i+1}^n \text{sign}(x_i - x_j), \text{sign} = \begin{cases} 1 & (\theta > 0) \\ 0 & (\theta = 0) \\ -1 & (\theta < 0) \end{cases}.$$

Where, Z is the standardized test statistic, and S is the test statistic. x_i and x_j are time series data; N is the sample number; When $n \geq 8$, S is approximately normal distribution, and the variance calculation formula is as follows:

$$\text{Var}(S) = \frac{n(n-1)(2n+5)}{18} \quad (3)$$

After standardization of Z is a standard normal distribution, when $|Z| > Z_{1-\alpha/2}$, showed significant change trend. Where, $Z_{1-\alpha/2}$ is the corresponding value of the distribution table of the standard normal distribution function at the confidence level α . Under the confidence level of 0.01 and 0.05 respectively in Mann Kendall test, three results: significant changes ($|Z| > 2.58$), significant changes ($|Z| > 1.96$) and no significant change ($-1.96 \leq |Z| \leq 1.96$) or less. Combined with the Theil-Sen trend analysis results and the MK test in $\alpha=0.05$ and $\alpha=0.01$, with the result of a sexual level can be divided into 6 level: will change significantly in 0.01 under the confidence level, 1) significantly improve ($S_{NDVI} \geq 0$, $|Z| > 2.58$); 2) significant degradation ($S_{NDVI} < 0$, $|Z| > 2.58$); In 0.05 under the confidence level, 3) improved significantly ($S_{NDVI} \geq 0$, $|Z| > 1.96$); 4) significant degradation ($S_{NDVI} < 0$, $|Z| > 1.96$); 5) does not significantly improve ($S_{NDVI} \geq 0$, $|Z| \leq 1.96$); 6) No significant retreat ($S_{NDVI} < 0$, $|Z| \leq 1.96$).

2.3.2. Geographically Weighted Regression Model

GWR model can analyze the data, the characteristic of spatial nonstationary and explore between vegetation change and its driving factors in spatial heterogeneity [6, 61, 62]. The kernel and bandwidth of the GWR model, which are key parameters affecting the accuracy of the model, are now generally determined by Gaussian kernel function, and the optimal bandwidth is generally determined based on the estimated distance of the spatial autocorrelation of the dependent variable [63]. In order to avoid multicollinearity, Variance Inflation Factor (VIF) was used to eliminate highly correlated variables from the model. In general, $VIF < 10$ had been commonly used to estimate the multicollinearity.

Usually in order to improve the accuracy of GWR model, using the general linear least-squares regression model, an Ordinary Least Squares regression (OLS) model is used for a preliminary inspection, inspection to check for multicollinearity among variables [34, 64].

Compared with OLS model, GWR can obtain more accurate estimation and provide more information. The GWR model is an extension of the traditional global logistic regression model, which includes spatial factors, geographic location information, and uses the weighted least square method to estimate the parameters of each sample point, so that each sample point has a corresponding estimation coefficient. Same as OLS model, assuming that the dependent variable (Slope of NDVI variation trend from 2000 to 2019 is represented by S_{NDVI}) is y , and the elevation, slope and aspect value are x_1 , x_2 , and x_3 respectively, the GWR model can be expressed as:

$$y = b_0(u_i, v_i) + \sum_{i=1}^k b_i(u_i, v_i) x_{ij} + \varepsilon \quad (4)$$

In the formula, (u_i, v_i) is the geographic coordinate center of a certain region, b_0 is a constant, b_i is the regression coefficient of independent variable, and x_{ij} is the independent variable.

The GWR model is constructed with the same variables as the OLS model in GWR4.0 software [65, 66], and the optimal bandwidth of 102 is determined according to the minimum *AIC* value to obtain the coefficient distribution of each variable. To facilitate the software analysis, we divided the study area into a 10 km × 10 km grid using the fishnet tool, obtaining a total of about 5000 sampling points, and extracted NDVI trend slope (S_{NDVI}), elevation, slope and aspect values for each sample point [66, 67].

3. Results

3.1. Spatial and Temporal Distribution Patterns of NDVI

The inter-annual variation analysis of NDVI during 2000-2019 revealed that NDVI values in the study area fluctuated between 0.56 and 0.61 in the past 20 years, with an overall growth rate of 0.007/10a ($P>0.05$), and from the viewpoint of each sub-basin, only the NDVI of Lancang river basin showed a significantly increasing trend ($P<0.05$) (Figure 3). Additionally, the results of M-K mutation analysis showed that the mutation of NDVI in the whole basin occurred in 2002, 2004 and 2008, respectively. Combining the NDVI mutations of each sub-basin, it was found that their NDVI mutations occurred simultaneously around 2004.

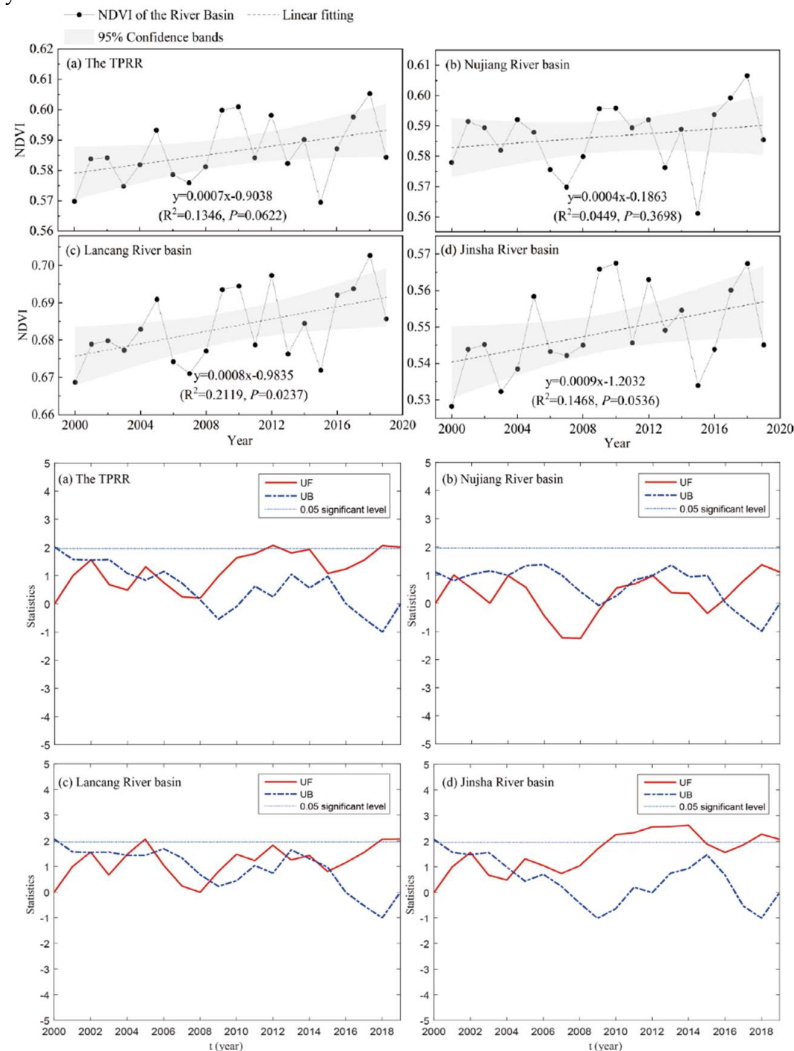


Figure 3. Inter-annual variation and Mann-Kendall test of NDVI in the basin from 2000 to 2019.

NDVI in the basin showed an initial increasing trend along a rising elevation (up to 4500 m) and eventually decreased (Figure 4a). The mean NDVI reached the maximum value (about 0.80) at the elevation of 3000m, and the lowest (about 0.05) above 5500m. Vegetation was mostly distributed within the elevation range of 1500-5500m. NDVI in the area with an elevation of less than 2500m is mostly above 0.75, which dominated by high vegetation cover, mainly distributed in the south of the study area, and the vegetation types were mainly cropland and evergreen coniferous forest (Table S2). Besides, from the spatial distribution of mean NDVI for different topographic factors (Figure S1a), the distribution range of vegetation is broader within the elevation of 2500-4500m with high NDVI value. The proportion of each grade indicated that areas dominated by high vegetation cover, are mostly spread over southern regions of the TPRR, especially in its core area (Figure 5a). However, a significant difference of vegetation cover appeared in the range of 4500-5000m, with greater middle and high vegetation areas in the south than in the north (31.16%). NDVI decreased gradually after reaching a certain elevation, with values close to 0.30 within the elevational range of 5000-5500 m for mainly low vegetation cover type (50.07%). At elevations above 5500m, NDVI values decreased further because climatic conditions rendered the region unfavorable for growth of vegetation, and vegetation type transitioned from low shrub to alpine meadow, and finally unvegetated snow-capped mountain tops.

With the increase of slope, NDVI showed an increasing trend with gradually slower growth rate (Figure 4b). The mean NDVI in the region with slope $<5^\circ$ was the lowest (0.40) and the NDVI for most of the region with slope $<5^\circ$ was between 0.05 and 0.3, with low vegetation cover mainly distributed in the north of the study area, and the main vegetation type was grassland (Figure 5b, Table S2). The NDVI for regions within the slope range of $5-8^\circ$ accounted for the largest proportion in the range of 0.6-0.75, mainly comprising of middle and high vegetation types. NDVI increased with the increasing of slope grades, and their distribution gradually shifted to the dry-hot valley. The mean NDVI reached its maximum value (about 0.80) at slope $>35^\circ$.

Furthermore, Figure 4c showed the NDVI changes with aspect from shady slope to sunny slope that the mean NDVI values were uniformly distributed in all aspects (approximately 0.60), and the smallest (about 0.01) existed on flat land. The proportion of high vegetation cover in each aspect was the largest (Figure 5c), which distribution pattern was relatively consistent. The brief descriptions were the proportion of high vegetation cover in semi-shady slope was the largest (35.25%), followed by semi-sunny slope, while the proportion of sunny slope was the smallest (27.83%) (Table S2).

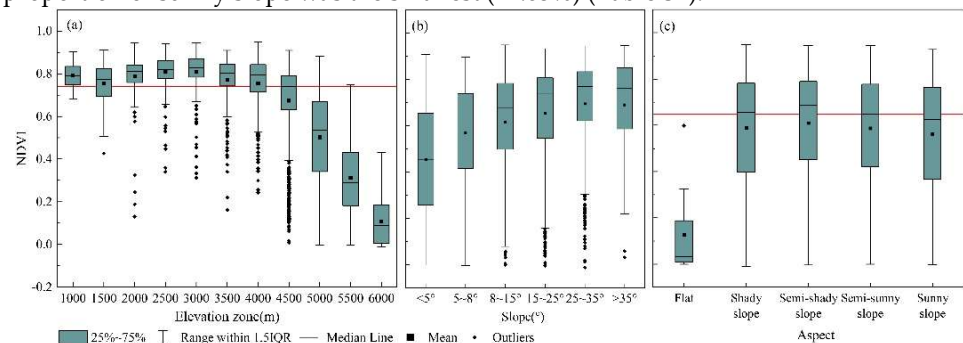


Figure 4. Variation characteristics of mean NDVI values in the TPRR with different topographic factors (a, b and c show elevation, slope and aspect respectively).

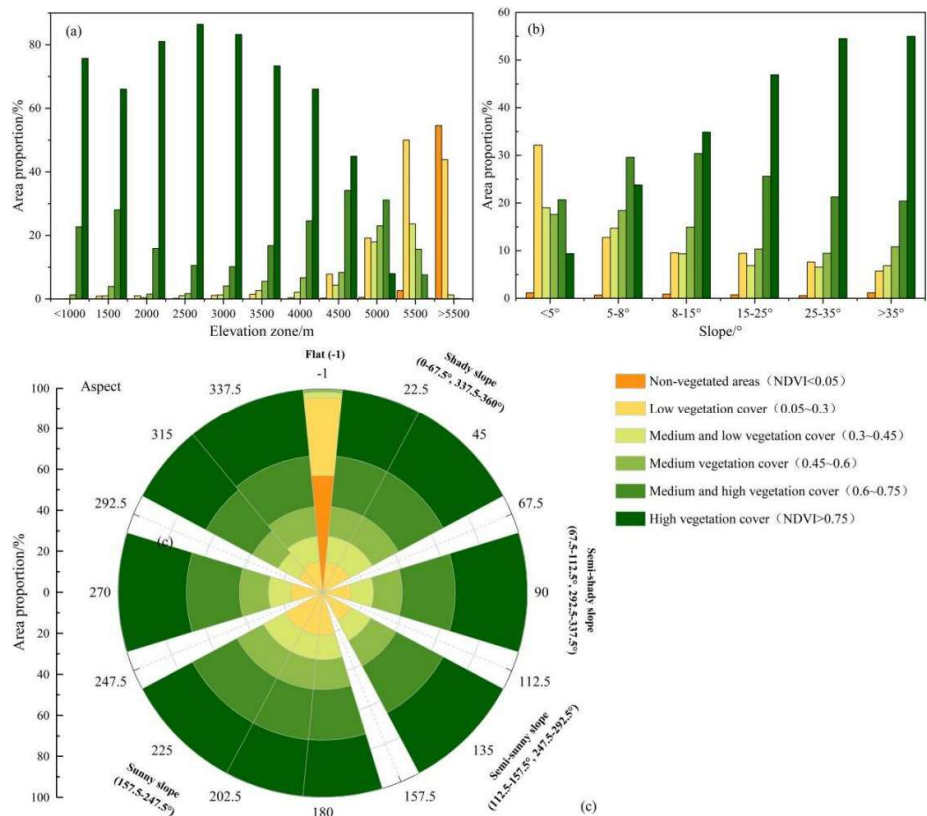


Figure 5. Area statistics of multi-year mean NDVI for topography factors during 2000-2019

3.2. Influence of Different Topographic Factors on the Variation Trend of NDVI

There was a significant spatial variation in NDVI of the TPRR from 2000 to 2019, showing that the vegetation cover in the basin had slightly improved (Figure 6). However, 31.74% of the region has not shown any change and 20.28% of the region showed slight degradation. Overall, the areas with improvement were mainly concentrated in the source area of Jinsha river basin in the north and the southern part of the TPRR. Meanwhile, degradation trends have primarily been observed in regions north of the Jinsha river basin and the valley of the TPRR as well as other areas with significant response to vegetation growth changes.

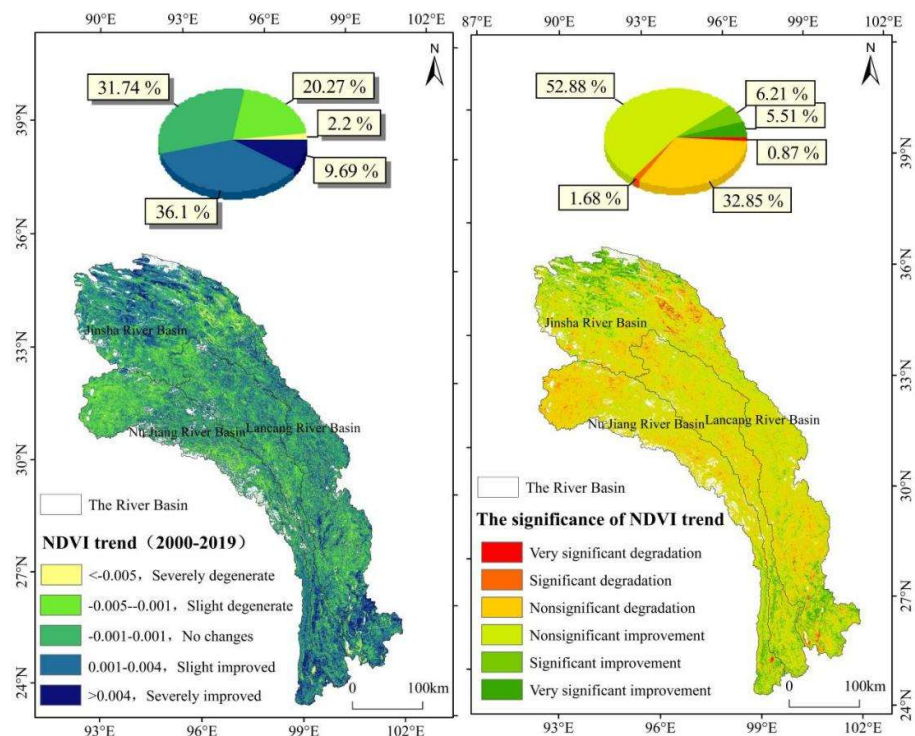


Figure 6. Spatial distribution of NDVI trend and significance during 2000-2019.

NDVI in the TPRR mostly showed an increasing trend under different topographic factors (Figure S2). Among them, NDVI values at all elevation zones showed an increasing trend except for regions above 5500m (Figure S2a), and we also observed that both slope and aspect did not play any significant role in determining NDVI trend distributional patterns (Figure S2b, Figure S2c).

More specifically, except for the three elevation zones, 3500-4000m, 4000-4500m and above 5500m, with the biggest proportion of no changes at 34.36%, 35.04%, and 43.81%, respectively, the majority of elevation zones (mainly 1000m-3500m) showed a slight improvement trend (Figure 7a, Table S3).

From the perspective of different slopes, approximately 35% of the area under all slope grades showed a slight improvement (Figure 7b, Table S3). With the increase of slope, the proportion of vegetation improvement area increased initially and eventually decreased. Among them, the slope in the northern part of the basin and the source area of TPRR was relatively small ($<5^\circ$), while the vegetation improvement trend was obvious, with grassland as mainly vegetation type (Figure S3a). The slope in the TPRR valley was mainly between 8° - 35° , where the main vegetation types were grassland and evergreen coniferous forest. The slope more than 35° in a few river valleys, especially in the Yunnan section of the TPRR, was dominated by evergreen coniferous forest. Besides, the proportion of improved areas (37.12%) was the largest in regions with 15° - 25° slope. However, we observed that the proportion of area with no changes decreased gradually with the increasing slope (Figure S3b).

According to different aspects, although there was little difference in the proportion of areas between vegetation improvement, stability and degradation, on an average we could witness slight improvement (Figure 7c, Table S3). Given that aspect had little influence on the vegetation variation trend in the basin, particularly on the variation of NDVI in flat land, the area proportion of vegetation improvement had an inconspicuous increasing trend from shady slope to sunny slope (Figure S3c).

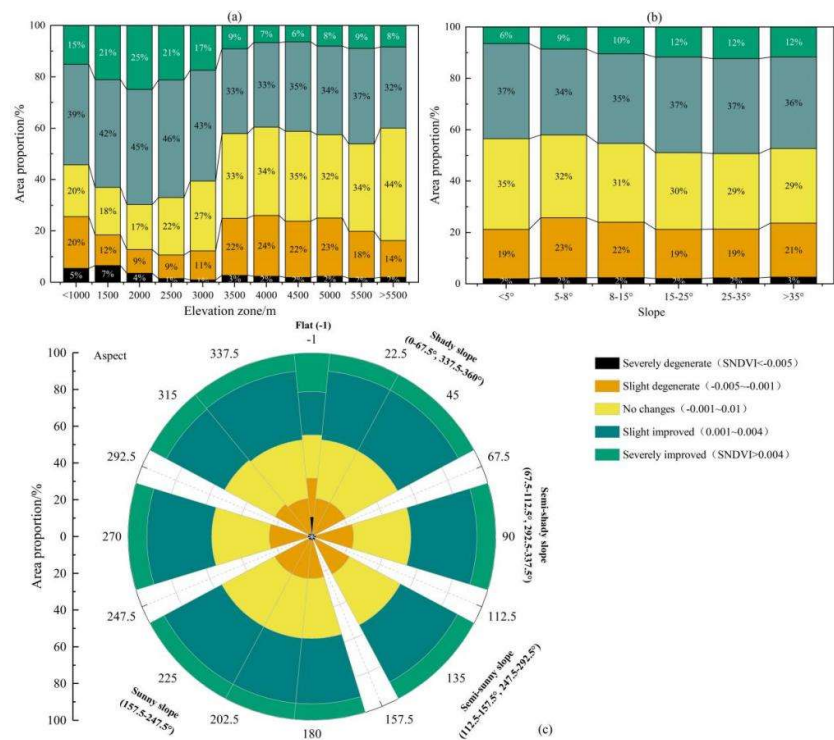


Figure 7. NDVI trend area statistics for different topographic factors from 2000 to 2019.

3.3. GWR-based Driving Force Analysis of vegetation change among different Basins

Taking S_{NDVI} as the dependent variable, and topographic factors (elevation, slope and aspect) as independent variables, the traditional multiple linear regression model based on OLS could not well explain the spatial heterogeneity of vegetation changes and topographic factors (Table S4; Figure S4; OLS model, $R^2 = 0.03$, $F = 60.76$), given variance inflation factors (VIF) of each variable were all less than 10.

However, GWR model provided a better overall fitting than OLS (Table 1, $R^2 = 0.33$), which is more proper than OLS in explaining vegetation changes. Moreover, the $AICc$ difference between GWR and OLS was much larger than 3 ($\Delta AICc = 1458.77$), indicating that the fit degree of GWR model is significantly higher than that of OLS, but the Residuals SS of the GWR model also decreases, which indicates that the fitting effect of the GWR model is greatly improved compared with the OLS model (Residuals $F = 4.31$) (Table S5).

Table1. Parameter estimation and test results of the GWR model.

Variable	Mean	Min	Max	Lwr Quartile	Median	Upr Quartile	SD
DEM	-1.13	-20.66	10.52	-1.97	-0.16	0.00	2.98
Slope	21.67	-580.16	824.38	-0.00	1.15	30.08	81.37
Aspect	0.04	-11.05	10.54	-0.55	0.00	0.53	2.35

The GWR model, as a local model, has a local set of parameter estimates at each sample data point, whereas the OLS model is only an estimate in a global or average sense. Based on the simulation results of the GWR model at the sampling points, we combined the IDW method to obtain the spatial variability characteristics of local parameter estimates and the significance level for different topographic factors (Figure 8).

The elevation in the headwaters of the TPRR (in particular, Nuijiang river and Jinsha river basins), the middle reaches of the Lancang river, and a few areas in the south of the TPRR (mainly in the south of the Jinsha river) has a significant positive correlation with S_{NDVI} , while the other vast majority of areas showed a negative correlation, e.g., the middle

reaches of Nujiang river and Jinsha river basin (Figure 8a). Slope also has a certain regularity on vegetation change since the slope steepness affects the soil and water conservation so that will directly affect the plant growth and development on the earth surface. Slope have both positive and negative effects on vegetation change in the study area given the influence intensity of slope on NDVI variation is much smaller than that of elevation. Among them, positive correlation trend mainly existed in the headwaters of the Jinsha river basin and a few areas in the middle reaches, the lower reaches of the Jinsha river and Nujiang river basins. However, there is a significant negative correlation trend between slope and vegetation variation trend in the junction of the Jinsha river and Nujiang river basins and a small part of the northwest of the source area in Jinsha river basin (Figure 8b). In terms of aspect, some significant positive correlations exist in a few source areas of the Nujiang river basin, a small part of the TPRR, as well as the junction of the south lower reaches between Jinsha river basin and Nujiang river basin given a significant negative correlation presented in some part of the Nujiang river basin and the source areas of the Jinsha river basin (Figure 8c).

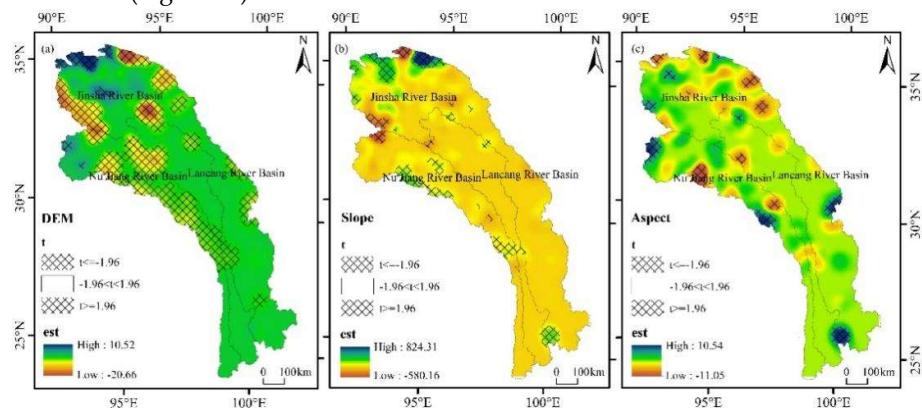


Figure 8. Spatial distribution maps of regression coefficients and significances for all independent variables. (Notes: (a) to (c) are the spatial distribution maps of the local regression coefficients and the significances for all independent variables, e.g., elevation, slope and aspect respectively.)

4. Discussion

4.1. Temporal and Spatial Distribution of Vegetation Patterns

Our results show that from 2000 to 2019, the vegetation in the TPRR shows an improving trend in a majority of the areas, while a few areas remain degraded, especially in the source areas of the entire Three Parallel Rivers basin where degradation is more obvious. Compared with the degraded areas, the proportion of areas with improved vegetation is much larger (45.79%). Our findings are consistent with those of other scholars in the Qinghai-Tibetan Plateau and TPRR, who also emphasized that vegetation dynamics in most areas of the Qinghai-Tibet Plateau have an upward trend, while some areas such as the Nagqu, a few areas in Qinghai Province and several areas on the southeastern edge of the QTP including the Hengduan Mountains are on a degradation trend. The combination of natural environmental changes and anthropogenic disturbances has increased vegetation degradation [18, 24]. Some scholars have studied vegetation pattern changes in the TPRR and showed that the significant reduction of vegetation cover was mainly in the source area of the Nujiang river and Lancang river as well as some areas in the central part of the study area, which corroborates with the findings of our study [20, 43]. Different vegetation types of mountainous vegetation are also significantly influenced by spatial scales [47, 68, 69]. With higher elevations in its northern region and relatively lower elevation in the southern regions the geographical structure in TPRR supports better vegetative growth in the southern region, with cropland and evergreen coniferous forest being main vegetation types. Most of the vegetation is distributed within the elevation range of

1500 to 5500 m, with a myriad of landscape and vegetation types overlaid and intertwined with one another [23]. Along an increasing elevational gradient, the vegetation types transition from subalpine forests, low scrub, alpine grassland to unvegetated areas. This variation in vegetation types is driven by topographic factors that alter regional hydrothermal conditions which in turn indirectly affect vegetation distribution [20, 46]. Peng et al. [24] showed the zonal characteristics of vegetation dynamics of different vegetation types, specifically the severe degradation of forests in the southeastern Tibetan Plateau, the increase of alpine grassland vegetation cover in some humid areas of southern Tibet, and the rising trend of cropland under the influence of agricultural activities in the Ali region and the plateau hinterland, all of which undoubtedly confirm the vegetation changes in our study area.

4.2. Spatial heterogeneity of topographic factors on Vegetation

The results of GWR model strengthen the intuitive perception of the spatial heterogeneity of different topographic factors on NDVI variation in the TPRR, with results indicating that elevation itself has the greatest influence on local vegetation patterns, followed by slope and aspect, which is consistent with previous studies [24, 26]. Altitude generally influences vegetation patterns by affecting mountain climate conditions [70, 71]. Our study area is in the Qinghai-Tibet Plateau region with large elevation differences, and the distribution of heat conditions is successively controlled by the law of decreasing elevation and solar radiation differences, while precipitation distribution mainly affected by the trend of water vapor channel orientation, which is mainly related to the distribution of mountains. Therefore, analyzing the influence of topographic factors on vegetation change can help in improving our understanding of the climate-vegetation change mechanism, which is often ignored in current research [72]. Notably, the relative importance of elevation is generally reflected in its effect on the gradient of species' ecological niches, which determines the type of vegetation distributed in the region and the growth of vegetation by representing laterally such environmental factors as slope or the amount of soil moisture [73, 74]. Besides, slope has been studied as a predictor variable to investigate plant diversity, and similarly, slope can capture potential changes in elevation in a region [73-76]. Slope can affect species richness by influencing soil moisture, soil erosion rates, and litter accumulation. However, related studies have shown that alpine treeline elevation changes in the Three Parallel Rivers region of southwest China are less affected by slope, further confirming the validity of our findings that slope has little effect on NDVI trends [39]. Finally, Yirdaw et al. suggested that aspect affected woody plant species diversity, especially for woody plants at higher elevations, and that sunny slopes tended to receive higher amounts of solar radiation, which could accelerate the increase in air and soil temperatures [27]. Nevertheless, our results indicate the effect of aspect on NDVI trend was not significant, which the highest vegetation cover (35.25%) was found on the semi-shady slopes. Few scholars have explored the effect of aspect on vegetation changes and even the distribution of some major species in our study area, which may require further research in this area.

4.3. Analysis of the Other Drivers Influencing Changes in Vegetation Dynamics

Beyond the influence of topographic factors on the vegetation pattern mentioned in this study, climatic conditions are the most well researched factor for vegetation change in the region. Studies have shown that temperature and precipitation indirectly affect the productivity of terrestrial ecosystems by altering nutrient availability [17, 77], and several scholars have reported the influence of climatic factors on vegetation changes in the Tibetan Plateau region, where temperature and precipitation affect the photosynthesis and respiration of vegetation by influencing soil moisture and microbial activity. There are obvious response mechanisms of temperature and precipitation on vegetation growth, but the effect of precipitation and temperature on vegetation degradation is not obvious

in a short period of time [26, 78, 79]. However, the direct influence of topography on climatic conditions in mountainous areas was mentioned in the previous subsection, and our study confirms the strong influence of elevation on vegetation distribution, but the relationship between topographic and climatic factors and the joint influence of both on vegetation distribution is lacking in this study area and needs further analysis.

In addition, the impact of human activities on the vegetation pattern should not be underestimated. Hengduan Mountain area in southeast Tibet act as a critical ecological barrier of the Qinghai-Tibet Plateau due to its unique ecological location and characteristics. In this region, several key national ecological projects have been implemented in the past to protect its natural forests, returning cropland to forest, biodiversity conservation, and ecological restoration, which have shown positive outcomes, and can also be the main reason for the improvement in NDVI observed in this study. Lu et al. (2015) compared the effects of three large-scale ecological programs (National Nature Reserves, Three North Shelter Forest Program, and the Natural Forest Protection Program) on Chinese vegetation change and revealed that the effectiveness of ecological restoration projects can vary geographically even under the same incentive policy context [80]. Moreover, several national and provincial protected areas, including the Three Parallel Rivers National Park, have been established in the TPRR. These protected areas can play a positive role in maintaining biodiversity, enhancing the regulation function of ecosystem, and building a scientific and reasonable ecological space. Grazing intensity is also one of the main driving factors affecting vegetation cover in grasslands on the Tibetan Plateau. Grasslands have been considered as natural pastures for grazing by herders for many years, especially in the Tibetan Plateau region [81, 82]. Studies have shown that long-term grazing directly affects the vegetation cover and productivity of grasslands on the Tibetan Plateau, but with the implementation of a series of ecological measures related to grassland restoration, e.g., rotation grazing prohibition, the degradation of grasslands has been mitigated, which may also be one of the main reasons why the vegetation trends in our study area tends to improve [83, 84].

5. Conclusions

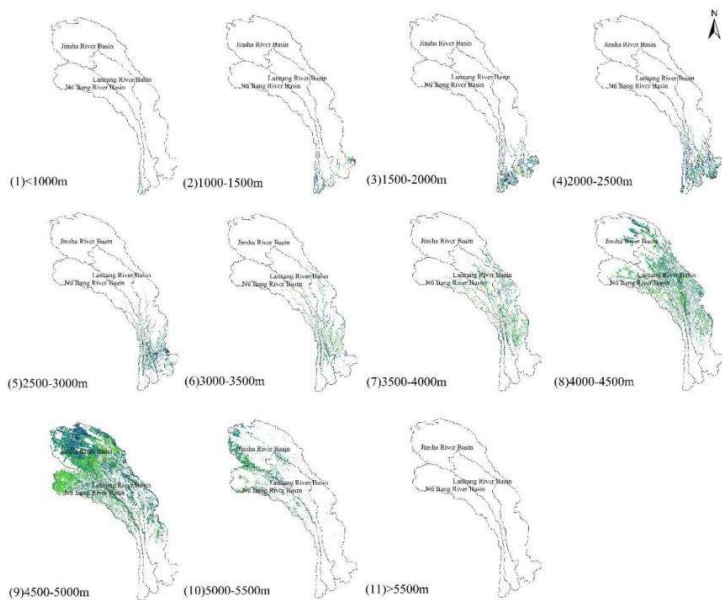
This study focused on the variation of vegetation pattern with topographic factors in the TPRR in the past 20 years by trend analysis and GWR model. During 2000-2019, NDVI of the study area showed an upward trend, with the most significant rising tendency in the Lancang river basin, where the common year of NDVI change in the whole basin and each sub-basin was around 2004. Besides, the distribution of mean NDVI was more related to elevation and less influenced by slope and aspect from 2000 to 2019. Specifically, there was a significant difference of NDVI between the northern regions (with less vegetation) as compared to the southern regions (covered with better vegetation) in the study area, since most of the vegetation types in the south are forests benefited from hydrothermal condition of Indian monsoon along the valleys. In addition, NDVI trend in the basin showed an overall improved trend with the different topographic factors, in which the slightly improved area accounted for the largest (36.10%). Spatially, the improved areas were mainly concentrated in the southern part of TPRR and the source area of the Jinsha river basin, while the degraded areas were concentrated in a few parts of the north Jinsha river basin and at the valley of the TPRR. Vegetation has slightly improved across most of the elevation zones (mainly 1000-3500m). The proportion of improved area increased initially and then decreased with increasing slope. Although aspects did not influence the NDVI much, slight improvement was observed. Furthermore, the GWR model showed that the elevation was negatively correlated with the vegetation changes in most areas but smaller effect of slope and aspect, significantly in a certain part of in the middle reaches of Nujiang river basin and Jinsha river basin.

Supplementary Materials:

Table S1. Classification of topographic factors in the study area.

Class	Elevation(m)	Proportion(%)	Slope(°)	Proportion (%)	Aspect	Proportion(%)
1	<1000m	0.23%	<5°	27.70%	Flat(-1)	0.30%
2	1000-1500m	1.22%	5-8°	11.36%	Shady slope (0-67. 5°, 337. 5-360°)	26.13%
3	1500-2000m	3.62%	8-15°	23.82%	Semi-shady slope (67. 5-112. 5°, 292. 5-337. 5°)	24.15%
4	2000-2500m	5.08%	15-25°	25.23%	Semi-sunny slope (112. 5-157. 5°, 247. 5-292. 5°)	23.87%
5	2500-3000m	4.31%	25-35°	10.40%	Sunny slope (157. 5-247. 5°)	25.55%
6	3000-3500m	4.35%	>35°	1.47%		
7	3500-4000m	7.07%				
8	4000-4500m	19.63%				
9	4500-5000m	42.76%				
10	5000-5500m	11.18%				
11	>5500m	0.55%				

a. Elevation



b. Slope

c. Aspect

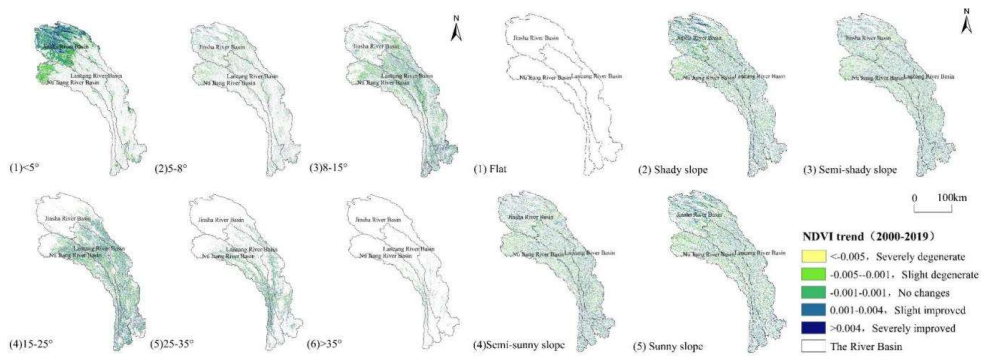


Figure S1. Spatial distribution of mean NDVI with different topographic factors during 2000-2019.

Table S2. Annual mean NDVI area statistics for different topographic factors during2000-2019.

Vegetation cover		Non-vegetated areas (NDVI<0.05)	Low vegetation cover (0.05~0.3)	Medium and low vegetation cover (0.3~0.45)	Medium vegetation cover (0.45~0.6)	Medium and high vegetation cover (0.6~0.75)	High vegetation cover (NDVI>0.75)
Topographic factors							
Elevation	<1000m	-	0.02%	0.11%	1.33%	22.76%	75.77%
	1000-1500m	-	0.89%	0.98%	3.99%	28.04%	66.10%
	1500-2000m	-	1.04%	0.42%	1.57%	15.91%	81.06%
	2000-2500m	-	0.23%	1.05%	1.72%	10.57%	86.44%
	2500-3000m	-	1.11%	1.27%	4.13%	10.22%	83.27%
	3000-3500m	-	1.53%	2.68%	5.58%	16.82%	73.39%
	3500-4000m	-	0.42%	2.17%	6.72%	24.63%	66.07%
	4000-4500m	0.25%	7.86%	4.38%	8.39%	34.19%	44.94%
	4500-5000m	0.54%	19.18%	18.03%	23.06%	31.16%	8.03%
	5000-5500m	2.69%	50.07%	23.67%	15.68%	7.65%	0.24%
	>5500m	54.63%	43.86%	1.33%	0.17%	0.01%	-
Slope	<5°	1.13%	32.15%	19.02%	17.62%	20.69%	9.38%
	5-8°	0.69%	12.75%	14.74%	18.44%	29.59%	23.80%
	8-15°	0.90%	9.52%	9.35%	14.96%	30.41%	34.87%
	15-25°	0.76%	9.45%	6.88%	10.37%	25.61%	46.93%
	25-35°	0.56%	7.59%	6.57%	9.48%	21.30%	54.50%
	>35°	1.18%	5.74%	6.86%	10.82%	20.43%	54.97%
Aspect	Flat	57.00%	38.57%	2.64%	1.09%	0.53%	0.18%
	Shady slope	0.88%	14.25%	12.39%	14.46%	24.74%	33.28%
	Semi-shady slope	0.76%	12.93%	11.20%	14.02%	25.83%	35.25%
	Semi-sunny slope	0.60%	15.05%	11.01%	14.05%	25.93%	33.36%
	Sunny slope	0.56%	20.40%	11.95%	14.54%	24.72%	27.83%

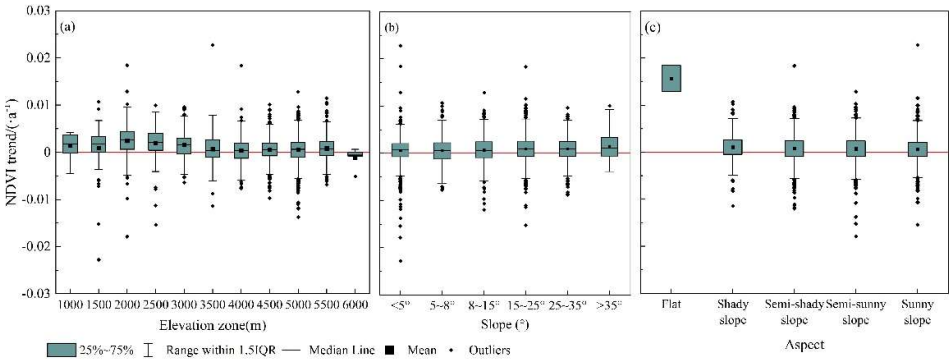


Figure S2. NDVI trends during 2000-2019 with different topographic factors in the basin (a, b, c show elevation, slope and aspect respectively).

a. Elevation

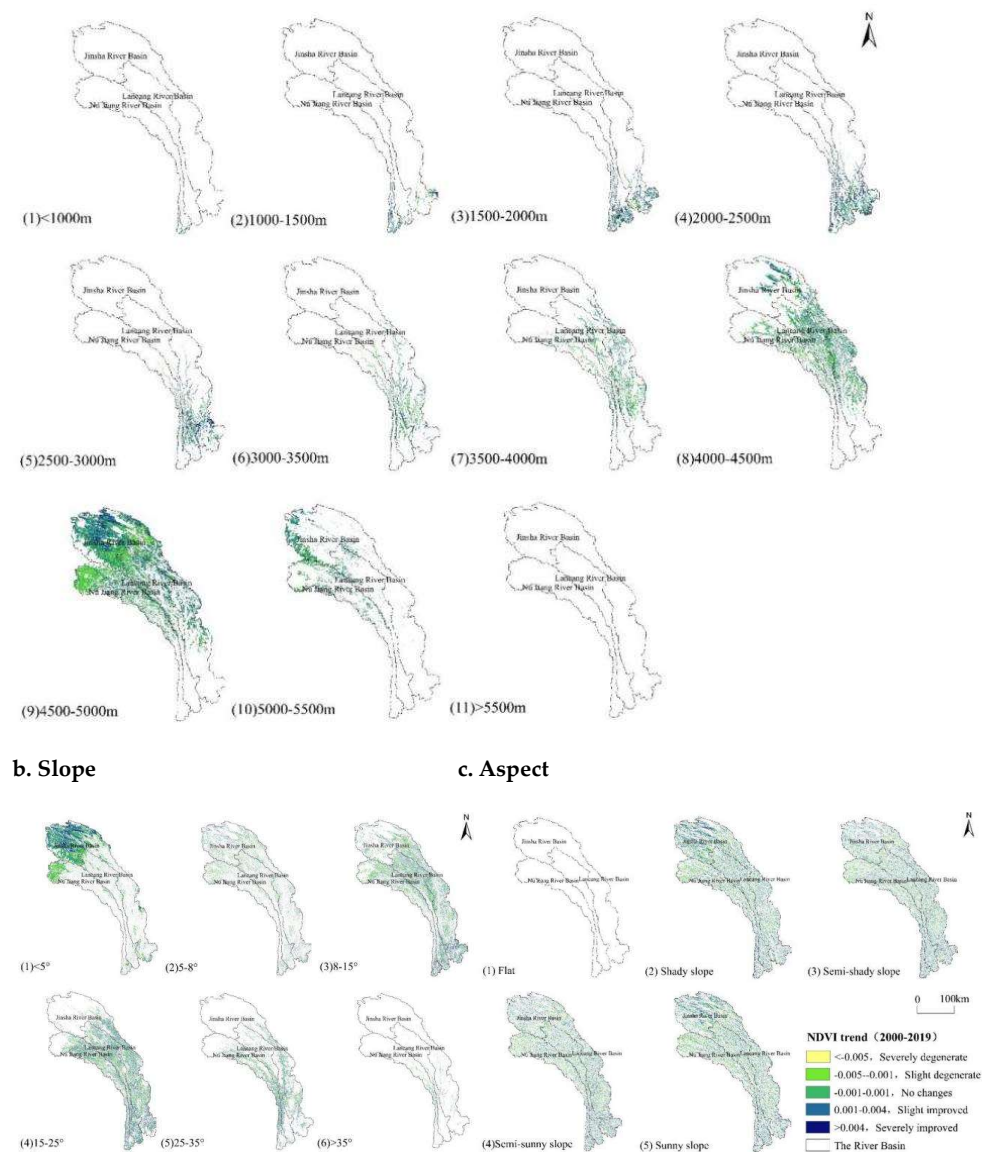


Figure S3. Spatial distribution of vegetation NDVI change trend of different topographic factors in the three parallel rivers basin from 2000 to 2019

Table S3. Area statistics of NDVI variation trends for different topographic factors from 2000 to 2019

Topographic factors	NDVI trend	Severely de- generate (SNDVI<-0.005)	Slight degen- erate (-0.005-0.001)	No changes (-0.001-0.01)	Slight improved (0.001-0.004)	Severely im- proved (SNDVI>0.004)
Elevation	<1000m	5.45%	20.14%	20.19%	39.13%	15.10%
	1000-1500m	6.51%	11.96%	18.49%	41.96%	21.07%
	1500-2000m	3.55%	9.24%	17.49%	44.78%	24.94%
	2000-2500m	1.47%	9.16%	22.41%	45.74%	21.22%
	2500-3000m	0.98%	11.29%	27.13%	43.14%	17.45%
	3000-3500m	2.70%	22.19%	32.97%	33.06%	9.08%
	3500-4000m	2.31%	23.72%	34.36%	32.90%	6.71%

	4000-4500m	1.92%	21.85%	35.04%	34.81%	6.39%
	4500-5000m	2.33%	22.69%	32.44%	34.48%	8.07%
	5000-5500m	1.62%	18.21%	34.04%	37.19%	8.93%
	>5500m	1.97%	14.28%	43.81%	31.57%	8.37%
Slope	<5°	1.97%	19.23%	35.30%	37.07%	6.43%
	5-8°	2.37%	23.38%	32.17%	33.50%	8.58%
	8-15°	2.37%	21.63%	30.65%	34.91%	10.44%
	15-25°	2.08%	19.11%	29.91%	37.12%	11.78%
	25-35°	2.31%	19.03%	29.41%	36.94%	12.32%
	>35°	2.60%	21.08%	28.98%	35.64%	11.70%
Aspect	Flat	10.86%	21.05%	23.46%	23.59%	21.05%
	Shady slope	1.86%	19.05%	31.97%	37.51%	9.60%
	Semi-shady slope	2.35%	20.46%	31.06%	35.93%	10.20%
	Semi-sunny slope	2.39%	20.88%	31.27%	35.25%	10.21%
	Sunny slope	2.23%	20.82%	32.53%	35.55%	8.88%

Table S4. Parameter estimation and test results of the OLS model

Variable	Dominant factors	Coefficient	Std Error	t-Statistic	Probability	VIF
Intercept	Constant term	1226.77	154.58	7.94	0.00***	-
X1	DEM	-0.41	0.03	-13.17	0.00***	1.07
X2	Slope	-1.65	3.17	-0.52	0.60	1.07
X3	Aspect	0.24	0.28	0.87	0.39	1.00

Note: *** indicates that the significance test at 1% level is passed.

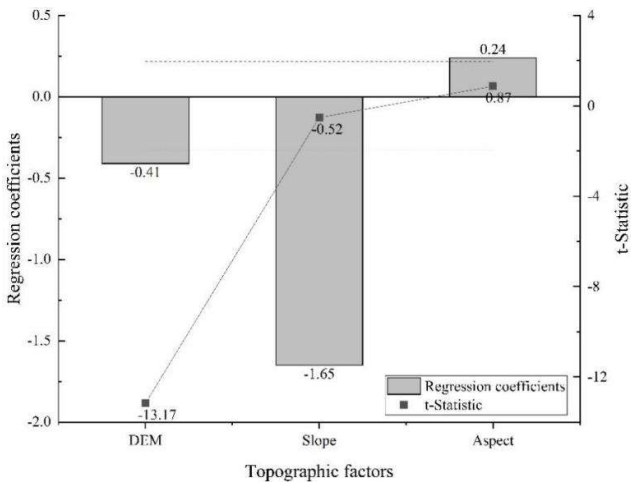


Figure S4. Estimation result of regression coefficients obtained through OLS modeling. (Notes: for the entire regression equation, the adjustment R^2 is 0.03, F value is 60.76, and $P < 0.01$; the two dashed lines denote that the t -value is equal to -1.96 and 1.96 respectively; at 0.05 significance level, $t < -1.96$ means a significantly negative correlation, while $t > 1.96$ represents a positive correlation.)

Table S5. Comparison of model performance between the GWR and OLS models.

Model parameters	AICc	R ²	Residuals SS	Residuals df	Adjusted R ²	Residuals MS	Residuals F
OLS	90394.77	0.04	20901792171.05	4994.00	0.03	-	-

GWR	88935.99	0.42	12545519136.66	4325.67	0.33	2900250.11	4.31
Improvement	1458.77	0.39	8356273034.39	668.33	-	-	-

Author Contributions: Conceptualization, J.W., N.W. and C.W.; methodology, C.W., X.C and Y.W.; software, C.W.; validation, J.W., and C.W.; formal analysis, C.W.; investigation, C.W.; resources, C.W.; data curation, C.W.; writing—original draft preparation, C.W.; writing—review and editing, C.W., J.W., N. N., N.W., X.C., Y.W. and Q.C.; visualization, C.W.; supervision, J.W.; project administration, J.W.; funding acquisition, J.W. All authors have read and agreed to the published version of the manuscript.

Funding: This research was funded by the National Science Foundation of China (No. 31971436 and 41661144045); State Key Laboratory of Cryospheric Science, Northwest Institute of Eco-Environment and Resources, Chinese Academy Sciences (SKLCSOP-2018-07) and China Biodiversity Observation Networks (Sino BON)“.

Data Availability Statement: The data presented in this study are available on request from the corresponding author.

Acknowledgments: The authors would like to thank the researchers who have provided the open-source algorithms, which have been extremely helpful to the research in this paper.

Conflicts of Interest: The authors declare no conflict of interest.

References

1. Wen, Z. F.; Wu, S. J.; Chen, J. L.; Lu, M. Q., NDVI indicated long-term interannual changes in vegetation activities and their responses to climatic and anthropogenic factors in the Three Gorges Reservoir Region, China. *Sci Total Environ* **2017**, *574*, 947-959.

2. Zhang, P. P.; Cai, Y. P.; Yang, W.; Yi, Y. J.; Yang, Z. F.; Fu, Q., Contributions of climatic and anthropogenic drivers to vegetation dynamics indicated by NDVI in a large dam-reservoir-river system. *J Clean Prod* **2020**, *256*.

3. Qu, S.; Wang, L. C.; Lin, A. W.; Zhu, H. J.; Yuan, M. X., What drives the vegetation restoration in Yangtze River basin, China: Climate change or anthropogenic factors? *Ecol Indic* **2018**, *90*, 438-450.

4. Julio Camarero, J.; Manzanedo, R. D.; Sanchez-Salguero, R.; Navarro-Cerrillo, R. M., Growth response to climate and drought change along an aridity gradient in the southernmost Pinus nigra relict forests. *Annals of Forest Science* **2013**, *70* (8), 769-780.

5. Palombo, C.; Marchetti, M.; Tognetti, R., Mountain vegetation at risk: Current perspectives and research needs. *Plant Biosystems* **2014**, *148* (1), 35-41.

6. Lu, L.; Xu, Y.; Huang, A.; Liu, C.; Marcos-Martinez, R.; Huang, L., Influences of Topographic Factors on Outcomes of Forest Programs and Policies in a Mountain Region of China: A Case Study. *Mountain Research and Development* **2020**, *40* (1), R48-R60.

7. Xu, M.; Ma, L.; Jia, Y.; Liu, M., Integrating the effects of latitude and altitude on the spatial differentiation of plant community diversity in a mountainous ecosystem in China. *Plos One* **2017**, *12* (3).

8. Grytnes, J.-A.; Kapfer, J.; Jurasinski, G.; Birks, H. H.; Henriksen, H.; Klanderud, K.; Odland, A.; Ohlson, M.; Wipf, S.; Birks, H. J. B., Identifying the driving factors behind observed elevational range shifts on European mountains. *Global Ecology and Biogeography* **2014**, *23* (8), 876-884.

9. Elliott, G. P., Extrinsic regime shifts drive abrupt changes in regeneration dynamics at upper treeline in the Rocky Mountains, USA. *Ecology* **2012**, *93* (7), 1614-1625.

10. Moyes, A. B.; Germino, M. J.; Kueppers, L. M., Moisture rivals temperature in limiting photosynthesis by trees establishing beyond their cold-edge range limit under ambient and warmed conditions. *New Phytologist* **2015**, *207* (4), 1005-1014.

11. Carbutt, C.; Edwards, T. J., Reconciling ecological and phytogeographical spatial boundaries to clarify the limits of the montane and alpine regions of sub-Saharan Africa. *South African Journal of Botany* **2015**, *98*, 64-75.

12. Hemp, A., Climate change-driven forest fires marginalize the impact of ice cap wasting on Kilimanjaro. *Global Change Biology* **2005**, *11* (7), 1013-1023.

13. Hertel, D.; Wesche, K., Tropical moist Polylepis stands at the treeline in East Bolivia: the effect of elevation on stand microclimate, above- and below-ground structure, and regeneration. *Trees-Structure and Function* **2008**, *22* (3), 303-315.
14. Monteiro, J. A. F.; Hiltbrunner, E.; Koerner, C., Functional morphology and microclimate of *Festuca orthophylla*, the dominant tall tussock grass in the Andean Altiplano. *Flora* **2011**, *206* (4), 387-396.
15. Klimes, L.; Dolezal, J., An experimental assessment of the upper elevational limit of flowering plants in the western Himalayas. *Ecography* **2010**, *33* (3), 590-596.
16. Koerner, C., Global Statistics of "Mountain" and "Alpine" Research. *Mountain Research and Development* **2009**, *29* (1), 97-102.
17. Körner, C., *Alpine Plant Life: Functional Plant Ecology of High Mountain Ecosystems*. Springer Nature Switzerland AG 2021
Springer-Verlag Berlin Heidelberg 1999, 2003 ed.; 2021.
18. Bohua, Y. U.; Changhe, L. U.; Tingting, L. U.; Aqiang, Y.; Chuang, L. I. U., Regional Differentiation of Vegetation Change in the Qinghai-Tibet Plateau. *Progress in Geography* **2009**, *28* (3), 391-397.
19. Guo, D.; Zhang, H. Y.; Hou, G. L.; Zhao, J. J.; Liu, D. Y.; Guo, X. Y., Topographic controls on alpine treeline patterns on Changbai Mountain, China. *J Mt Sci-Engl* **2014**, *11* (2), 429-441.
20. Liu, X. F.; Zhang, J. S.; Zhu, X. F.; Pan, Y. Z.; Liu, Y. X.; Zhang, D. H.; Lin, Z. H., Spatiotemporal changes in vegetation coverage and its driving factors in the Three-River Headwaters Region during 2000-2011. *J Geogr Sci* **2014**, *24* (2), 288-302.
21. Wang, B.; Xu, G.; Li, P.; Li, Z.; Zhang, Y.; Cheng, Y.; Jia, L.; Zhang, J., Vegetation dynamics and their relationships with climatic factors in the Qinling Mountains of China. **2020**, 108.
22. Zoungrana, B. J. B.; Conrad, C.; Thiel, M.; Amekudzi, L. K.; Da, E. D., MODIS NDVI trends and fractional land cover change for improved assessments of vegetation degradation in Burkina Faso, West Africa. *J Arid Environ* **2018**, *153*, 66-75.
23. Jian, P.; You, L.; Lu, T.; Yanxu, L.; Yanglin, W., Vegetation Dynamics and Associated Driving Forces in Eastern China during 1999–2008. *Remote Sensing* **2015**, *7* (10), 13641-13663.
24. Peng, J.; Liu, Z.; Liu, Y.; Wu, J.; Han, Y., Trend analysis of vegetation dynamics in Qinghai–Tibet Plateau using Hurst Exponent. *Ecol Indic* **2012**, *14* (1), 28-39.
25. Xu, M.; Li, X.; Liu, M.; Shi, Y.; Zhou, H.; Zhang, B.; Yan, J., Spatial variation patterns of plant herbaceous community response to warming along latitudinal and altitudinal gradients in mountainous forests of the Loess Plateau, China. *Environmental and Experimental Botany* **2020**, 172.
26. Wang, H.; Qi, Y.; Huang, C.; Li, X.; Deng, X.; Zhang, J., Analysis of vegetation changes and dominant factors on the Qinghai-Tibet Plateau, China. *Sciences in Cold and Arid Regions* **2019**, *11* (2), 150-158.
27. Yirdaw, E.; Starr, M.; Negash, M.; Yimer, F., Influence of topographic aspect on floristic diversity, structure and treeline of afro-montane cloud forests in the Bale Mountains, Ethiopia. *Journal of Forestry Research* **2015**, *26* (4), 919-931.
28. Mohapatra, J.; Singh, C. P.; Tripathi, O. P.; Pandya, H. A., Remote sensing of alpine treeline ecotone dynamics and phenology in Arunachal Pradesh Himalaya. *International Journal of Remote Sensing* **2019**, *40* (20), 7986-8009.
29. Jacquin, A.; Sheeren, D.; Lacombe, J.-P., Vegetation cover degradation assessment in Madagascar savanna based on trend analysis of MODIS NDVI time series. *International Journal of Applied Earth Observation and Geoinformation* **2010**, *12*, S3-S10.
30. Gao, Q. Z.; Ganjurjav, Li, Y.; Wan, Y. F.; Zhang, W. N.; Borjigday, A., Challenges in disentangling the influence of climatic and socio-economic factors on alpine grassland ecosystems in the source area of Asian major rivers. *Quatern Int* **2013**, *304*, 126-132.
31. Sun, Y. L.; Yang, Y. L.; Zhang, Y.; Wang, Z. L., Assessing vegetation dynamics and their relationships with climatic variability in northern China. *Phys Chem Earth* **2015**, *87-88*, 79-86.
32. Zewdie, W.; Csaplovics, E.; Inostroza, L., Monitoring ecosystem dynamics in northwestern Ethiopia using NDVI and climate variables to assess long term trends in dryland vegetation variability. *Appl Geogr* **2017**, *79*, 167-178.

33. Ren, Y.; Lu, Y.; Fu, B.; Comber, A.; Li, T.; Hu, J., Driving Factors of Land Change in China's Loess Plateau: Quantification Using Geographically Weighted Regression and Management Implications. *Remote Sensing* **2020**, *12* (3).
34. Brunsdon, C.; Fotheringham, A. S.; Charlton, M. E., Geographically Weighted Regression: A Method for Exploring Spatial Nonstationarity. **1996**, *28* (4), 281-298.
35. Dullinger, S.; Dirnbock, T.; Grabherr, G., Modelling climate change-driven treeline shifts: relative effects of temperature increase, dispersal and invasibility. *J Ecol* **2004**, *92* (2), 241-252.
36. Diao, Y. X.; Wang, J. J.; Yang, F. L.; Wu, W.; Zhou, J.; Wu, R. D., Identifying optimized on-the-ground priority areas for species conservation in a global biodiversity hotspot. *J Environ Manage* **2021**, 290.
37. Liang, J.; Liu, Y.; Ying, L.; Li, P.; Xu, Y.; Shen, Z., Road impacts on spatial patterns of land use and landscape fragmentation in three parallel rivers region, Yunnan Province, China %J Chinese Geographical Science. **2014**, *24* (1).
38. Ou, X.; Replumaz, A.; van der Beek, P., Contrasting exhumation histories and relief development within the Three Rivers Region (south-east Tibet). *Solid Earth* **2021**, *12* (3), 563-580.
39. Wang, W.; Körner, C.; Zhang, Z.; Wu, R.; Geng, Y.; Shi, W.; Ou, X., No slope exposure effect on alpine treeline position in the Three Parallel Rivers Region, SW China %J Alpine Botany. **2013**, *123* (2).
40. Li H, Zhao K, Zhu X, et al. Protecting and using of ecotourism resource of moon mountain scenic spot in Three Parallel River Area[J]. *Ecological Economy*, **2008**, (5): 75-80.
41. Guo Y, Yang F L, Wang J J, Wu R D. Assessment of the tourism and recreation cultural ecosystem services in Three Parallel Rivers Region. *Acta Ecologica Sinica*, **2020**, *40* (13) :4351-4361.
42. Guo, Y.; Wu, R.; Yang, F.; Wang, J., The spatial patterns of scenic spots in Three Parallel Rivers Region. *Journal of Yunnan University. Natural Science* **2020**, *42* (5), 992-1003.
43. Pan, X.; Wu, X.; Shen, Y.; Liu, F.; Zhang, C., Responses of Vegetation Coverage Changes to Climate Factors in the Source Regions of Three Parallel Rivers. *Mountain Research* **2015**, *33* (2), 218-226.
44. Deng, C.; Zhang, W., Spatiotemporal distribution and the characteristics of the air temperature of a river source region of the Qinghai-Tibet Plateau. *Environ Monit Assess* **2018**, *190* (6), 368.
45. Huang, C.; Li, Y. F.; Liu, G. H.; Zhang, H. L.; Liu, Q. S., Recent climate variability and its impact on precipitation, temperature, and vegetation dynamics in the Lancang River headwater area of China. *International Journal of Remote Sensing* **2014**, *35* (8), 2822-2834.
46. Li, J. P.; Dong, S. K.; Peng, M. C.; Li, X. Y.; Liu, S. L., Vegetation distribution pattern in the dam areas along middle-low reach of Lancang-Mekong River in Yunnan Province, China. *Front Earth Sci-Pre* **2012**, *6* (3), 283-290.
47. Cheng, Z. J.; Weng, C. Y.; Guo, J. Q.; Dai, L.; Zhou, Z. Z., Vegetation responses to late Quaternary climate change in a biodiversity hotspot, the Three Parallel Rivers region in southwestern China. *Palaeogeogr Palaeocl* **2018**, *491*, 10-20.
48. Yao, X.; Deng, J.; Liu, X.; Zhou, Z.; Yao, J.; Dai, F.; Ren, K.; Li, L., Primary Recognition of Active Landslides and Development Rule Analysis for Pan Three-river-parallel Territory of Tibet Plateau. *Advanced Engineering Sciences* **2020**, *52* (5), 16-37.
49. Gao, Y.; Zhao, S.; Deng, J., Developing Law of Damming Landslide and Challenges for Disaster Prevention and Mitigation in the Three-river-parallel Territory in the Tibetan Plateau. *Advanced Engineering Sciences* **2020**, *52* (5), 50-61.
50. Myers, N.; Mittermeier, R. A.; Mittermeier, C. G.; da Fonseca, G. A. B.; Kent, J., Biodiversity hotspots for conservation priorities. *Nature* **2000**, *403* (6772), 853-858.
51. China, M. o. W. R. t. P. s. R. o., Standards for classification and gradation of soil erosion. **2008**.
52. He, W.; Ye, C.; Sun, J.; Xiong, J.; Wang, J.; Zhou, T., Dynamics and Drivers of the Alpine Timberline on Gongga Mountain of Tibetan Plateau-Adopted from the Otsu Method on Google Earth Engine. *Remote Sensing* **2020**, *12* (16).
53. Jiang, L.; Liu, X.; Feng, Z., Remote Sensing Identification and Spatial Pattern Analysis of the Alpine Timberline in the Three Parallel Rivers Region. *Resources Science* **2014**, *36* (2), 259-266.

54. Yang, Y. K.; Xiao, P. F.; Feng, X. Z.; Li, H. X., Accuracy assessment of seven global land cover datasets over China. *Isprs J Photogramm* **2017**, *125*, 156-173.
55. Kuppel, S.; Fan, Y.; Jobbagy, E. G., Seasonal hydrologic buffer on continents: Patterns, drivers and ecological benefits. *Adv Water Resour* **2017**, *102*, 178-187.
56. Gang, C. C.; Zhao, W.; Zhao, T.; Zhang, Y.; Gao, X. R.; Wen, Z. M., The impacts of land conversion and management measures on the grassland net primary productivity over the Loess Plateau, Northern China. *Sci Total Environ* **2018**, *645*, 827-836.
57. Bontemps, S.; Boettcher, M.; Brockmann, C.; Kirches, G.; Lamarche, C.; Radoux, J.; Santoro, M.; Vanbogaert, E.; Wegmüller, U.; Herold, M.; Achard, F.; Ramoino, F.; Arino, O.; Defourny, P., Multi-year global land cover mapping at 300 m and characterization for climate modelling: achievements of the Land Cover component of the ESA Climate Change Initiative %J ISPRS - International Archives of the Photogrammetry, Remote Sensing and Spatial Information Sciences. **2015**, *XL-7/W3* (1), 323-328.
58. Gregory, D.; Josh, H.; Alessandro, C., A dataset mapping the potential biophysical effects of vegetation cover change. . %J *Scientific data* **2018**, *5*.
59. Liu, J.; Wen, Z.; Gang, C., Normalized difference vegetation index of different vegetation cover types and its responses to climate change in the Loess Plateau. *Acta Ecologica Sinica* **2020**, *40* (2), 678-691.
60. Li, H.; Xie, M.; Wang, H.; Li, S.; Xu, M., Spatial Heterogeneity of Vegetation Response to Mining Activities in Resource Regions of Northwestern China. *Remote Sensing* **2020**, *12* (19).
61. Zhi, Y.; Shan, L.; Ke, L.; Yang, R., Analysis of Land Surface Temperature Driving Factors and Spatial Heterogeneity Research Based on Geographically Weighted Regression Model. *Complexity* **2020**, *2020*.
62. Comber, A. J.; Brunsdon, C.; Radburn, R., A spatial analysis of variations in health access: linking geography, socio-economic status and access perceptions. *International Journal of Health Geographics* **2011**, *10* (1), 44.
63. Yang, C.; Li, R.; Sha, Z., Exploring the Dynamics of Urban Greenness Space and Their Driving Factors Using Geographically Weighted Regression: A Case Study in Wuhan Metropolis, China. *Land* **2020**, *9* (12).
64. Zhao, R.; Yao, M.; Yang, L.; Qi, H.; Meng, X.; Zhou, F., Using geographically weighted regression to predict the spatial distribution of frozen ground temperature: a case in the Qinghai-Tibet Plateau. *Environmental Research Letters* **2021**, *16* (2).
65. Nakaya, T. GWR4.09 user manual. WWW Document [online]. Available from: https://raw.githubusercontent.com/gwr-tools/gwr4/master/GWR4manual_409.pdf.
66. Zhang, D.; Jia, Q.; Wang, P.; Zhang, J.; Hou, X.; Li, X.; Li, W., Analysis of spatial variability in factors contributing to vegetation restoration in Yan'an, China. *Ecol Indic* **2020**, *113*.
67. Xue, R.; Yu, X.; Li, D.; Ye, X., Using geographically weighted regression to explore the effects of environmental heterogeneity on the space use by giant pandas in Qinling Mountains. *Acta Ecologica Sinica* **2020**, *40* (8), 2647-2654.
68. Levin, S. A., The Problem of Pattern and Scale in Ecology: The Robert H. MacArthur Award Lecture. **1992**, *73* (6), 1943-1967.
69. Zhang, W. J.; Liu, L.; Song, K. C.; Li, X. D.; Wang, Y. D.; Tang, Y.; Jiang, H. R., Remote sensing the orographic effects of dry-hot valley on vegetation distribution in the southeast Tibetan Plateau. *International Journal of Remote Sensing* **2019**, *40* (22), 8589-8607.
70. Grytnes, J. A., Species-richness patterns of vascular plants along seven altitudinal transects in Norway. *Ecography* **2003**, *26* (3), 291-300.
71. Lenoir, J.; Graae, B. J.; Aarrestad, P. A.; Alsos, I. G.; Armbruster, W. S.; Austrheim, G.; Bergendorff, C.; Birks, H. J. B.; Brathen, K. A.; Brunet, J.; Bruun, H. H.; Dahlberg, C. J.; Decocq, G.; Diekmann, M.; Dynesius, M.; Ejrnaes, R.; Grytnes, J.-A.; Hylander, K.; Klanderud, K.; Luoto, M.; Milbau, A.; Moora, M.; Nygaard, B.; Odland, A.; Ravolainen, V. T.; Reinhardt, S.; Sandvik, S. M.; Schei, F. H.; Speed, J. D. M.; Tveraaabak, L. U.; Vandvik, V.; Velle, L. G.; Virtanen, R.; Zobel, M.; Svenning, J.-C., Local temperatures inferred from plant communities suggest strong spatial buffering of climate warming across Northern Europe. *Global Change Biology* **2013**, *19* (5), 1470-1481.

72. White, A. B.; Kumar, P.; Tcheng, D., A data mining approach for understanding topographic control on climate-induced inter-annual vegetation variability over the United States. *Remote Sensing of Environment* **2005**, *98* (1), 1-20.
73. Jia, L.; Li, Z.-b.; Xu, G.-c.; Ren, Z.-p.; Li, P.; Cheng, Y.-t.; Zhang, Y.-x.; Wang, B.; Zhang, J.-x.; Yu, S., Dynamic change of vegetation and its response to climate and topographic factors in the Xijiang River basin, China. **2020**, *27* (2).
74. Moeslund, J. E.; Arge, L.; Bocher, P. K.; Dalgaard, T.; Odgaard, M. V.; Nygaard, B.; Svenning, J. C., Topographically controlled soil moisture is the primary driver of local vegetation patterns across a lowland region. *Ecosphere* **2013**, *4* (7).
75. Jones, M. M.; Szyska, B.; Kessler, M., Microhabitat partitioning promotes plant diversity in a tropical montane forest. *Global Ecology and Biogeography* **2011**, *20* (4), 558-569.
76. Zhang, C. S.; Li, X. Y.; Chen, L.; Xie, G. D.; Liu, C. L.; Pei, S., Effects of Topographical and Edaphic Factors on Tree Community Structure and Diversity of Subtropical Mountain Forests in the Lower Lancang River Basin. *Forests* **2016**, *7* (10).
77. Jobbágy, E. G.; Sala, O. E.; Paruelo, J. M., Patterns and Controls of Primary Production in the Patagonian Steppe: A Remote Sensing Approach. *Ecology* **2002**, *83* (2), 307-319.
78. Mou, X. M.; Yu, Y. W.; Li, X. G.; Degen, A. A., Presence frequency of plant species can predict spatial patterns of the species in small patches on the Qinghai-Tibetan Plateau. *Global Ecology and Conservation* **2020**, *21*.
79. Sun, J.; Cheng, G. W.; Li, W. P., Meta-analysis of relationships between environmental factors and aboveground biomass in the alpine grassland on the Tibetan Plateau. *Biogeosciences* **2013**, *10* (3), 1707-1715.
80. Lu, Y.; Zhang, L.; Feng, X.; Zeng, Y.; Fu, B.; Yao, X.; Li, J.; Wu, B., Recent ecological transitions in China: greening, browning, and influential factors. *Scientific Reports* **2015**, *5*.
81. Cao, J.; Adamowski, J. F.; Deo, R. C.; Xu, X.; Gong, Y.; Feng, Q., Grassland Degradation on the Qinghai-Tibetan Plateau: Reevaluation of Causative Factors. *Rangeland Ecology & Management* **2019**, *72* (6), 988-995.
82. Liu, Y.; Liu, S.; Sun, Y.; Li, M.; An, Y.; Shi, F., Spatial differentiation of the NPP and NDVI and its influencing factors vary with grassland type on the Qinghai-Tibet Plateau. *Environmental Monitoring and Assessment* **2021**, *193* (1).
83. Zhang, W. N.; Ganjurjav, H.; Liang, Y.; Gao, Q. Z.; Wan, Y. F.; Li, Y.; Baima, Y. Z.; Xirao, Z. M., Effect of a grazing ban on restoring the degraded alpine meadows of Northern Tibet, China. *Rangeland J* **2015**, *37* (1), 89-95.
84. Fayiah, M.; Dong, S.; Li, Y.; Xu, Y.; Gao, X.; Li, S.; Shen, H.; Xiao, J.; Yang, Y.; Wessell, K., The relationships between plant diversity, plant cover, plant biomass and soil fertility vary with grassland type on Qinghai-Tibetan Plateau. *Agriculture Ecosystems & Environment* **2019**, *286*.